Binding affinities and protein ligand complex geometries of nucleotides at the F_1 part of the mitochondrial ATP synthase obtained by ligand docking calculations

Thomas Steinbrecher[a], Oliver Hucke[a], Stefan Steigmiller[a], Michael Börsch[a,b], Andreas Labahn[a,*]

[a] *Institut für Physikalische Chemie der Albert-Ludwigs-Universität Freiburg, Albertstraße 23a, D-79104 Freiburg, Germany*
[b] *3. Physikalisches Institut der Universität Stuttgart, Pfaffenwaldring 57, 70550 Stuttgart, Germany*

Received 14 August 2002; accepted 6 September 2002

First published online 23 September 2002

Edited by Vladimir Skulachev

Abstract **F_0F_1 ATP synthases utilize a transmembrane electrochemical potential difference to synthesize ATP from ADP and phosphate. In this work, the binding modes of ADP, ATP and ATP analogues to the catalytic sites of the F_1 part of the mitochondrial ATP synthase were investigated with ligand docking calculations. Binding geometries of ATP and ADP at the three catalytic sites agree with X-ray crystal data; their binding free energies suggest an assignment to the 'tight', 'open' and 'loose' states. The rates of multi-site hydrolysis for two fluorescent ATP derivatives were measured using a fluorescence assay. Reduced hydrolysis rates compared to ATP can be explained by the ligand docking calculations.**

Key words: ATP synthase; Ligand docking; Fluorescent ATP derivatives

1. Introduction

A crucial step in the energy metabolism of the cell is the conversion of potential energy stored in an electrochemical potential gradient of protons across the membrane to chemical energy in the form of ATP synthesized from ADP and inorganic phosphate, P_i. The coupling of the proton flux with ATP synthesis is performed by the F_0F_1 ATP synthase.

This ubiquitous enzyme is a multi-subunit membrane protein complex consisting of two distinct domains, the intramembraneous F_0 part and the hydrophilic F_1 part, which performs ATP synthesis. The subunit composition of F_0 and F_1 depends on the organism. However, in all species the F_1 part contains a core of $\alpha_3\beta_3\gamma$ subunits. Several X-ray crystal structures exist for the mitochondrial F_1 part [1–8]. The α and β subunits are arranged alternately to form a pseudo-hexamer, while the γ subunit occupies the center of the $\alpha_3\beta_3$ assembly. Three catalytic and three non-catalytic nucleotide binding sites are located on the αβ interfaces of the F_1 part.

According to the binding change mechanism [9], the catalytic binding sites exist in three different states, named 'open', 'loose' and 'tight'. During catalysis, one catalytic site passes through all three states, while at any time each catalytic site is in a different state than the other two. This interconversion of states is believed to be accomplished by the rotation of the rod-like γ subunit within the globular $\alpha_3\beta_3$ assembly. Evidence for this amazing mechanism was found in numerous experiments [10–12], making the ATP synthase a mechanoenzyme or nanomachine.

The three states of the catalytic sites reveal markedly different binding affinities to ATP, ADP and various nucleotide analogues, which were used to study the enzyme (reviewed in [13]). In this work, we present the calculated binding free energies and complex geometries of ATP and ADP at the catalytic binding sites. Furthermore, docking calculations with the photo-cleavable analogue 'caged ATP', which was used in numerous kinetic measurements with other ATPases [14–16], were performed as well as calculations with two fluorescent ATP derivatives useful for single-molecule spectroscopy.

2. Materials and methods

2.1. Ligand docking algorithm

The docking calculations were performed with FlexX, a program designed for the docking of small to medium sized organic molecules into protein binding sites [17]. During the docking procedure, the protein is considered rigid, whereas the ligand conformation is flexible by allowing rotations around acyclic single bonds of the ligand structure and by considering multiple possible conformers for ring structures. Bond lengths and angles are kept constant as given in the input structure. A relatively soft atom model is used by FlexX to compensate for the rigidity of the binding site, i.e. small overlap of the ligand with the receptor is tolerated by the program.

The docking algorithm incorporated in FlexX is based on matching complementary functional groups like H-bond donors and acceptors. It favors sterically restrictive interactions like salt bridges and H-bonds. The ligand is not placed into the binding site as a whole. It is broken down into a special fragment, the so-called base fragment, and into a set of additional fragments, each connected to the rest of the ligand by a rotatable single bond. The first placement step is carried out with the base fragment. In the subsequent placement steps the ligand is built up fragment by fragment, ranking the different placements of the partial ligand according to their calculated binding free energy and considering only the highest ranked placements in the following step. The binding free energy is calculated with an empiri-

*Corresponding author. Fax: (49)-761-203 6189; http://pc2-em6.physchem.uni-freiburg.de/Andreas/homepage.
E-mail address: andreas.labahn@physchem.uni-freiburg.de (A. Labahn).

Abbreviations: MF_1, F_1 part of the mitochondrial F_0F_1 ATP synthase; EF_1, F_1 part of the F_0F_1 ATP synthase from *E. coli*; BODIPY-FL-ATP, adenosine 5′-triphosphate, BODIPY® FL 2′-(or-3′)-*O*-(*N*-(2-aminoethyl) urethane); BODIPY-TR-ATP, adenosine 5′-triphosphate, BODIPY® TR 2′-(or-3′)-*O*-(*N*-(2-aminoethyl) urethane)

0014-5793/02/$22.00
PII: S0014-5793(02)03433-6

cally derived scoring function, based on the Böhm function [18]. The algorithm is described in detail in [17,19].

Depending on the number of possible ligand conformations, the docking calculations resulted in a set of up to 100 predicted protein ligand complexes per ligand. FlexX ranks these solutions according to their calculated binding free energies. Unless stated otherwise, only the best placement ('placement 1'), displaying the most negative value of the binding free energy, was considered for further analysis.

2.2. Ligand docking procedure

The catalytic binding sites of the ATP synthase were determined with the program InsightII (Accelrys). The X-ray structures were taken from the Protein Data Bank (PDB) [20]. All amino acids from an X-ray crystal structure (PDB code 1E1Q [3]) with at least one atom lying within 8.5 Å of any atom of a bound nucleotide were considered to be part of the corresponding binding pocket[1]. Using a larger binding site had no effect on the results of the calculations. In the X-ray structure several water molecules were found within the binding sites. Only water molecules tightly bound to the receptor were considered in the docking calculations. Tight binding of a water molecule to the receptor was judged by three criteria: its crystallographic B-value, the number of strong H-bonds being formed to the protein and the occurrence of a water molecule at the same coordinates in other X-ray crystal structures of the F_1 part of the mitochondrial F_0F_1 ATP synthase (MF_1)[2]. The number of H-bonds was determined with the program package WhatIf [21], the occurrence of water molecules in other X-ray structures with the program MODELLER [22].

FlexX uses a united atom model for all non-polar hydrogen atoms, whereas polar protons are explicitly taken into consideration. Where unambiguously clear, the positions of the protons in the protein binding site were automatically assigned by FlexX. In cases of ambiguities (hydrogens of the hydroxyl groups of Ser, Thr or Tyr, the N-bound proton of histidine side chains and the protons of water molecules), they were determined with WhatIf.

The geometries of the ligands were optimized with the MM+ force field of the Hyperchem software (Hypercube) prior to use as input files for the docking calculations. The program FlexX does not allow metal ions to be part of the ligands. Because of that, the Mg^{2+} ions found in the X-ray crystal structure were considered part of the receptor during the docking calculations and the binding free energies of the Mg^{2+} complexed nucleotides were calculated using a simple thermodynamic cycle:

$$\Delta G_{\mathrm{Mg-Nu}} = \Delta G_{\mathrm{Nu}} + \Delta G_{\mathrm{Mg-Rec}} - \Delta G_{\mathrm{Mg-Li}} \quad (1)$$

$\Delta G_{\mathrm{Mg-Nu}}$ is the binding free energy of a nucleotide including a bound Mg^{2+} to the binding pocket at the receptor, ΔG_{Nu} is the binding free energy of the Mg^{2+}-free nucleotide to the receptor with bound Mg^{2+}, $\Delta G_{\mathrm{Mg-Rec}}$ represents the binding free energy of the Mg^{2+} to the receptor and $\Delta G_{\mathrm{Mg-Li}}$ is that of the Mg^{2+} to the ligand nucleotide. $\Delta G_{\mathrm{Mg-Rec}}$ and $\Delta G_{\mathrm{Mg-Li}}$ were determined from the output of the docking calculations. $\Delta G_{\mathrm{Mg-Nu}}$ and ΔG_{Nu} are very similar in all calculations, differing only by ~1 kJ/mol. For the catalytic binding site without a Mg^{2+} in the X-ray structure, the calculations were carried out without Mg^{2+} ion. Placing a Mg^{2+} into that binding site before the docking calculations with InsightII did not yield satisfactory docking results.

To perform a more detailed search of the ligand's conformational space, the program parameter SOL_PER_IT was set to 1000, instead of the default 500. This parameter determines how many possible conformations of the ligand are considered in each placement step. For the placement of the base fragment of the ligand the perturbation mode was used, which creates an ensemble of placements around a given set of starting coordinates. In the calculations both the ribose and the nucleotide residue of the ligands were used as base fragments. Only the solution with the lowest binding free energy from both dockings was considered further. As starting coordinates for the placement of the base fragment, the coordinates of the corresponding parts of the ligands from the X-ray crystal structure were used.

2.3. Measurements of ATP hydrolysis

For measurements of ATP hydrolysis rates, the F_1 part of the F_0F_1 ATP synthase from *Escherichia coli* (EF_1) was prepared as described earlier [23] and stored at −80°C. The continuous measurement of ATP hydrolysis was carried out in an UV/VIS spectrometer (Perkin Elmer Lambda 2) at 37°C by detecting the decrease of NADH at 340 nm in an enzymatic coupled assay containing 2.0 mM ATP and 0.2 mM NADH [24]. This assay could not be used to measure ATP hydrolysis rates of the fluorescent nucleotide analogues. Instead, we used the following approach. An aliquot of 0.8 μl of 5 mM adenosine 5′-triphosphate, BODIPY® FL 2′-(or-3′)-*O*-(*N*-(2-aminoethyl) urethane) (BODIPY-FL-ATP, Molecular Probes) or 5 mM adenosine 5′-triphosphate, BODIPY® TR 2′-(or-3′)-*O*-(*N*-(2-aminoethyl) urethane) (BODIPY-TR-ATP, Molecular Probes) was dissolved in 39 μl buffer (50 mM HEPES, 2.5 mM $MgCl_2$, pH = 8.0). Both ATP derivatives were contaminated with ~10% of the corresponding ADP analogues. To start the reaction, 0.2 μl of EF_1 (20 μM) was added; the ratio of nucleotide to enzyme amounted to 1000:1. Reactions were stirred at 37°C and monitored by thin layer chromatography on non-fluorescent silica gel TLC plates (Macherey-Nagel) using 2-propanol:water:ammonium hydroxide (70:20:10) as the mobile phase. Reaction samples (0.3 μl) were taken at 15 s intervals. The spots were treated by heat gun for several seconds in order to denature the enzyme and to stop the reaction. BODIPY-FL-ATP migrated with an R_f value of 0.02, whereas the hydrolysis product BODIPY-FL-ADP showed an R_f value of 0.10. BODIPY-TR-ATP and BODIPY-TR-ADP displayed R_f values of 0.03 and 0.10, respectively. Developed plates were imaged by UV-illumination at 365 nm, digitally photographed and quantified by Adobe Photoshop software (Adobe Systems). Therefore, the fluorescence of the single spots was separated into their green, red and blue intensity components with 8-bit resolution. The ratio of BODIPY-FL-ATP and BODIPY-FL-ADP was measured by analyzing the green intensity over 25 pixels after subtraction of background intensity. The ratio of BODIPY-TR-ATP and BODIPY-TR-ADP was determined by analyzing the red channel intensities.

3. Results and discussion

The docking calculations with the natural substrates of the ATP synthase, ATP and ADP, exhibited markedly different binding affinities of both nucleotides to the three different binding sites. Table 1 summarizes the calculated binding free energies and classifies some of their components. The total binding free energies show that ATP is more tightly bound to the catalytic binding sites than ADP.

The ΔG values for the ATP molecules bound to the β_{TP} and β_{DP} sites differ by 11 kJ/mol, for those bound to the β_{TP} and β_E sites they differ by 15 kJ/mol. This is equal to a change in the dissociation constant by a factor of 85 and 426, respectively ($T = 298$ K). For ADP these differences of the binding free energies are smaller, 7 kJ/mol and 5 kJ/mol, corresponding to changes in the dissociation constants by a factor of 17 and 8, respectively.

Experimental binding constants obtained from measurements with EF_1 [13] correspond well to these data, although the calculations were performed with MF_1. In the area of the binding pockets ~90% of the amino acids are identical, making it likely that the binding properties are very similar. As in the calculations, three markedly different binding constants for ATP were found and the differences between the binding constants in consecutive binding of three ATP molecules were greater than those for the binding of three ADP molecules.

Based on the different components in the scoring function of FlexX, we deduced that the major component of the

[1] In one catalytic binding site only a phosphate ion is located. To compensate for the smaller ligand, here a distance of 15 Å from any atom of the phosphate ion was used to determine the amino acids forming this binding site.

[2] The structures with the PDB codes 1BMF [1], 1E1R [3], 1E79 [4], 1EFR [5], 1H8H [6] and 1NBM [8] were used.

Table 1
Calculated binding free energies for ATP and ADP

Ligand	Binding site	ΔG_{Total} [kJ/mol]	ΔG_{Iact} [kJ/mol]	ΔG_{Lipo} [kJ/mol]	ΔG_{Clash} [kJ/mol]	ΔG_{PPP} [kJ/mol]	Important residues
ATP	β_{TP}	−75	−74	−11	7	−65	αArg 373, βArg 189, βLys 162
ATP	β_{DP}	−86	−83	−12	6	−67	αArg 373, βArg 189, βLys 162
ATP	β_{E}	−60	−71	−4	5	−59	αArg 373, βArg 189, βArg 260
ADP	β_{TP}	−45	−46	−9	6	−41	αArg 373, βArg 189, βLys 162
ADP	β_{DP}	−52	−48	−10	4	−38	βLys 162
ADP	β_{E}	−40	−48	−5	5	−36	βLys 162, βArg 189, βArg 260

The nomenclature of the binding sites was chosen as in [1]. ΔG_{Total} is the calculated total binding free energy. ΔG_{Iact} is the part of ΔG_{Total} that is caused by H-bonds, salt bridges and metal – metal ligand bonds. ΔG_{Lipo} is the part of ΔG_{Total} caused by lipophilic constants, e.g. van der Waal's interactions between hydrophobic atoms. ΔG_{Clash} is a penalty factor for overlap of receptor and ligand, ΔG_{PPP} is the part of the binding free energy that is caused by interactions of the pyrophosphate/triphosphate residue of the ligand with the receptor. Amino acid residues that participate in interactions which contribute to a large amount of binding free energy to ΔG_{Total} are listed.

binding free energy are sterically restrictive interactions of H-bonds and salt bridges. The triphosphate chain of ATP and the pyrophosphate residue of ADP contribute to more than 80% of the total interaction energy in all calculations. For each docked ligand, amino acid residues can be identified which form strong interactions with the ligand (Table 1). These amino acids interact with the phosphate groups (Fig. 1). It is notable that in all calculations with ATP the amino acid residue αArg 373 is found to form such strong interactions. This is consistent with the proposal that this residue participates in the binding of the substrates [1]. On the ligand side, the oxygen atom bridging the β- and γ-phosphate residue participates in the H-bonds. It was suggested that αArg 373 is important for the stabilization of the intermediate state during catalysis [3].

The calculations show for ATP and ADP a ΔG contribution of lipophilic contacts in the range of 10 kJ/mol for the β_{TP} and β_{DP} binding sites, but only about half that value for the β_{E} site. Due to the hydrophilic nature of the ribose and the phosphate groups, this ΔG contribution can be assigned to the adenine residues of the ligands. This means that the β_{E} binding pocket does not offer a matching hydrophobic surface, probably because the hydrophobic adenine binding pocket described in [1] is not formed in that conformation.

The ΔG penalty for overlap of receptor and ligand atoms, ΔG_{Clash}, is in all six calculations 4–7 kJ/mol, less than 10% of the total ΔG value. This indicates that the ligands fit well into the binding sites, or that only small conformational changes of the protein are necessary to remove any overlap between ligand and receptor.

By comparing the calculated protein ligand complex geometries to the geometries of the cocrystallized ligands, it is evident that the docking solutions superimpose well with the coordinates from the X-ray structure (Fig. 1). The rmsd values are 1.1 Å for ATP in the β_{TP} binding site, 1.2 Å for ATP in the β_{DP} binding site. For ADP the values are 1.7 Å and 1.2 Å, respectively. For the β_{E} binding site no rmsd value can be quoted, because no nucleotide is found there in the X-ray structure.

The docking calculations with the ATP derivative γ-P-(2-

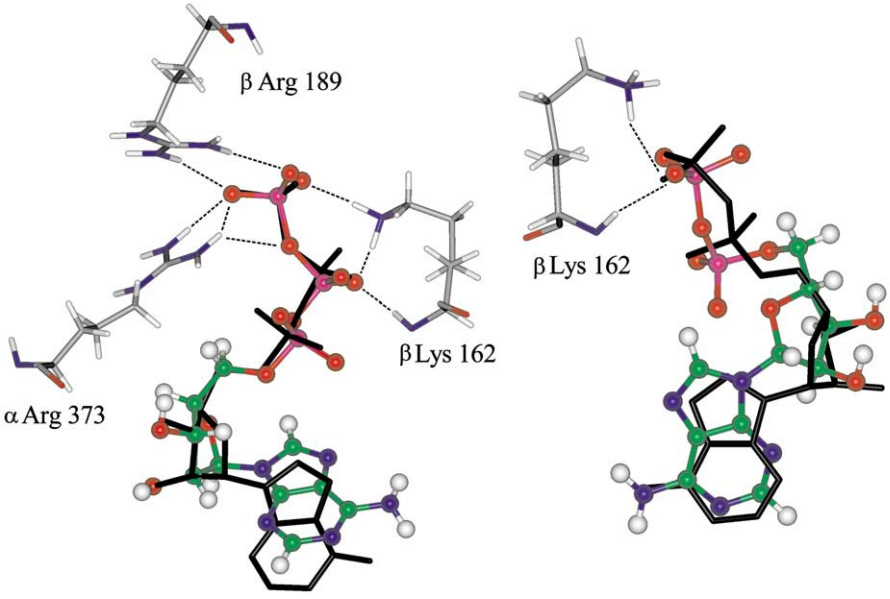

Fig. 1. The binding geometries of ATP at the β_{TP} (left) and ADP at the β_{DP} (right) binding site of MF_1. The ligand coordinates from the X-ray structure [3] are depicted in black, whereas the docked ligand and amino acids forming important interactions are colored by atom type. The nitrogen, oxygen, phosphorus, hydrogen, ligand carbon and amino acid carbon atoms are drawn in blue, red, violet, white, green and gray, respectively. The docked ligand is drawn as ball and stick, the amino acids in stick representation. Important ligand protein interactions are shown as black dotted lines.

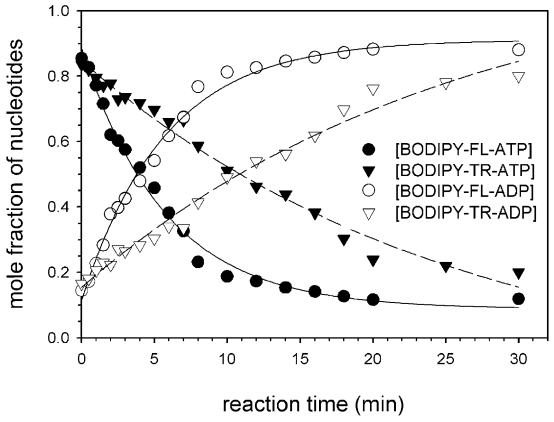

Fig. 2. Hydrolysis rates of ATP derivates. Circles show the reaction of BODIPY-FL-nucleotides, triangles the reaction of BODIPY-TR-nucleotides. The hydrolysis of the ATP derivatives is shown by filled symbols, the corresponding increase of the ADP derivatives by open symbols. The curves were fitted with monoexponential functions providing the rates of ATP hydrolysis (R_H). For BODIPY-TR-ATP and BODIPY-FL-ATP the rates were found to be 2.5 s^{-1} and 7.2 s^{-1}, respectively, which is considerably smaller than that of the native MgATP ($R_H = 33$ s^{-1}).

nitro)-benzyladenosyl-5′-triphosphate ('caged ATP') revealed possible binding geometries for this ligand. However, several facts make it unlikely that the calculated geometries for the β_{TP} and β_{DP} binding sites represent reasonable binding modes in vivo. Though the calculated geometries are very similar to that of ATP[3], the computed ΔG values are ~20 kJ/mol more positive than those for ATP at either site. For 'caged ATP' docked to the β_{TP} binding site, only three possible docking solutions were found, much less than for the native substrates. Furthermore, the predicted binding geometries have ΔG_{Clash} values of 13 kJ/mol for both sites, which is about twice the value of the native substrates. These data suggest that 'caged ATP' is either not bound to the β_{TP} and β_{DP} sites, or that these binding sites undergo conformational deviations from the X-ray structure to accommodate the ligand.

Rates of ATP hydrolysis (R_H) were measured for the fluorescent ATP analogues BODIPY-FL-ATP and BODIPY-TR-ATP with EF_1 ATPase. Compared to $R_H = 33$ s^{-1} for MgATP at an enzyme concentration of 100 nM ($T = 37$°C), the rates of the hydrolysis reaction are reduced (Fig. 2). For BODIPY-FL-ATP, the rate is reduced by a factor of 4.5 ($R_H = 7.2$ s^{-1}), but this nucleotide is still hydrolyzed under multi-site conditions where all three binding sites are used. BODIPY-TR-ATP is also hydrolyzed by EF_1, but the rate is further reduced to one third of the value found for the BODIPY-FL derivative ($R_H = 2.5$ s^{-1}).

The docking calculations with these fluorescent ATP derivatives showed that they bind to the β_E and β_{TP} binding sites with reasonable binding geometries and ΔG values (−53 to −95 kJ/mol). However, at the β_{DP} site, no complex geometries were found for BODIPY-FL-ATP. For BODIPY-TR-ATP, only two solutions with severely reduced binding free energies (−55 kJ/mol, compared to −86 for ATP) and ΔG_{Clash} values of ~20 kJ/mol were found for this binding site. This might explain the reduced hydrolysis rates of these fluorescent ATP analogues. If they do not fit into all of the conformations that a binding site adopts during catalysis, the mechanism of their hydrolysis must either include conformational adaptations of the binding site or differ from that proposed in the binding change mechanism.

The results of the docking calculations with ATP and ADP suggest an assignment of the three conformations of the catalytic binding sites to the 'open', 'loose' and 'tight' states according to the binding change mechanism [9]. The calculated ΔG values allow to identify the β_{DP} binding site as the 'tight', the β_{TP} as the 'loose' and the β_E as the 'open' binding site. This assignment, together with the fact that the γ subunit rotates counterclockwise during ATP hydrolysis when viewed from the F_0 part [10], leads to the conclusion that the sequence of states that a binding site adopts during ATP synthesis is open–tight–loose as proposed by Boyer [25] but in contrast to the model of Cross in [26].

Our results show that the X-ray crystal structures of MF_1 can be used for ligand docking calculations to help in elucidating the interactions of the ATP synthase with various substrates on a molecular level. The fact that the reduced rates of hydrolysis for the fluorescent ATP derivatives can be explained by the results of the docking calculations demonstrates that the program FlexX is well-suited to enable the design of new nucleotide analogues for kinetic studies of the ATP synthase.

Acknowledgements: We thank Professor Dr. P. Gräber for his constant support of our work.

References

[1] Abrahams, J.P., Leslie, A.G., Lutter, R. and Walker, J.E. (1994) Nature 370, 621–628.
[2] van Raaij, M.J., Abrahams, J.P., Leslie, A.G. and Walker, J.E. (1996) Proc. Natl. Acad. Sci. USA 93, 6913–6917.
[3] Braig, K., Menz, R.I., Montgomery, M.G., Leslie, A.G.W. and Walker, J.E. (2000) Structure 8, 567–573.
[4] Gibbons, C., Montgomery, M.G., Leslie, A.G.W. and Walker, J.E. (2000) Nat. Struct. Biol. 7, 1055–1061.
[5] Abrahams, J.P., Buchanan, S.K., van Raaij, M.J., Fearnley, I.M., Leslie, A.G. and Walker, J.E. (1996) Proc. Natl. Acad. Sci. USA 93, 9420–9424.
[6] Menz, R.I., Leslie, A.G.W. and Walker, J.E. (2001) FEBS Lett. 494, 11–14.
[7] Menz, R.I., Walker, J.E. and Leslie, A.G.W. (2001) Cell 106, 331–341.
[8] Orriss, G.L., Leslie, A.G.W., Braig, K. and Walker, J.E. (1998) Structure 6, 831–837.
[9] Boyer, P.D. (1975) FEBS Lett. 58, 1–6.
[10] Noji, H., Yasuda, R., Yoshida, M. and Kinosita, K. (1997) Nature 386, 299–302.
[11] Zhou, Y., Duncan, T.M. and Cross, R.L. (1997) Proc. Natl. Acad. Sci. USA 94, 10583–10587.
[12] Börsch, M., Diez, M., Zimmermann, B., Reuter R. and Gräber, P. (2002) in: Fluorescence Spectroscopy, Imaging and Probes: New Tools in Chemical, Physical and Life Sciences (Kraayenhof, R., Visser, A.J.W.G., Gerritsen, H.C., Eds.), pp. 197–207, Springer, Heidelberg, Germany.
[13] Weber, J. and Senior, A.E. (1997) Biochim. Biophys. Acta 1319, 19–58.
[14] Higuchi, H., Muto, E., Inoue, Y. and Yanagida, T. (1997) Proc. Natl. Acad. Sci. USA 94, 4395–4400.
[15] Lewis, S.M. and Thomas, D.D. (1991) Biochemistry 30, 8331–8339.
[16] Ferenczi, M.A. and Spencer, I.C. (1988) Adv. Exp. Med. Biol. 226, 181–188.

[3] The rmsd values of placement 1 at the two binding sites compared to the cocrystallized nucleotides are 1.3 Å for the β_{TP} and 1.2 Å for the β_{DP} site.

[17] Rarey, M., Kramer, B., Lengauer, T. and Klebe, G. (1996) J. Mol. Biol. 261, 470–489.
[18] Böhm, H. (1994) J. Comput.-Aided Mol. Des. 8, 243–256.
[19] Rarey, M., Kramer, B. and Lengauer, T. (1999) Bioinformatics 15, 243–250.
[20] Berman, H.M., Westbrook, J., Feng, Z., Gilliland, G., Bhat, T.N., Weissig, H., Shindyalov, I.N. and Bourne, P.E. (2000) Nucleic Acids Res. 28, 235–242.
[21] Vriend, G. (1990) J. Mol. Graph. 8, 52–56.
[22] Sali, A. and Blundell, T.L. (1993) J. Mol. Biol. 234, 779–815.
[23] Gogol, E.P., Lücken, U., Bork, T. and Capaldi, R.A. (1989) Biochemistry 28, 4709–4716.
[24] Rosing, J., Harris, D.A., Kemp, A.J. and Slater, E.C. (1975) Biochim. Biophys. Acta 376, 13–26.
[25] Boyer, P.D. (2000) Biochim. Biophys. Acta 1458, 252–262.
[26] Cross, R.L. (2000) Biochim. Biophys. Acta 1458, 270–275.